A High Level Ab Initio Study of the Anionic Hydrogen-Bonded Complexes FH···CN⁻, FH···NC⁻, H_2O···CN⁻ and H_2O···NC⁻

Timothy J. Lee†

University Chemical Laboratory, Lensfield Road, Cambridge CB2 1EW, United Kingdom

and

ELORET Institute, Sunnyvale, California 94087, USA

Abstract

HF, H_2O, CN^- and their hydrogen-bonded complexes have been studied using state-of-the-art *ab initio* quantum mechanical methods. A large Gaussian one-particle basis set consisting of triple zeta plus double polarization plus diffuse s and p functions (TZ2P + diffuse) was used. The theoretical methods employed include self-consistent-field, second-order Møller-Plesset perturbation theory, singles and doubles configuration interaction theory and the singles and doubles coupled cluster approach. The FH···CN^-, FH···NC^- and H_2O···CN^-, H_2O···NC^- pairs of complexes are found to be essentially isoenergetic. The first pair of complexes are predicted to be bound by $\sim$ 24 kcal/mole and the latter pair bound by $\sim$ 15 kcal/mole. The *ab initio* binding energies are in good agreement with the experimental values. The two pairs of complexes exhibit small structural differences with the N···H hydrogen bond being shorter than the analogous C···H hydrogen bond. The infrared (IR) spectra of the two pairs of complexes are also very similar, though a severe perturbation of the potential energy surface by proton exchange means that the accurate prediction of the band center of the most intense IR mode requires a high level of electronic structure theory as well as a complete treatment of anharmonic effects. The bonding of anionic hydrogen-bonded complexes is discussed and contrasted with that of neutral hydrogen-bonded complexes.

---

† NATO/NSF Postdoctoral Fellow. Mailing Address: NASA Ames Research Center, Moffett Field, California 94035

Introduction

Over the past sixty years, hydrogen-bonded complexes have attracted considerable attention from chemists. Much of the interest has been directed at the understanding of the nature of the relatively weak bonding present in neutral hydrogen-bonded complexes. To this end, several different hydrogen bonding decomposition schemes have been developed. The basis for the classical description of hydrogen bonding was presented in a review[1] by Coulson in 1957. The classical hydrogen bond energy is decomposed into four distinct components - (1) the electrostatic energy; (2) the delocalization energy (commonly referred to as the charge transfer energy); (3) the repulsive energy and (4) the dispersion energy. Since Coulson limited his review to hydrogen-bonded complexes involving a polar molecule containing an electronegative atom (such as N, O or F) and a molecule containing a polar A-H bond (where A = N, O or F), the electrostatic interaction is viewed as the dominant attractive force. For some Van der Waals complexes Morokuma and coworkers have demonstrated[2-4] that the electrostatic energy may be very small or even represent a repulsive force. However, for most hydrogen-bonded complexes the electrostatic interaction will be attractive. The dispersion energy also represents an attractive force and thus, in Coulson's review, the "repulsive force" is the only interaction which separates monomers A and B. The explanation of the physical nature of this "repulsive force" is based, not surprisingly, on electron-electron repulsion, i.e. the mutual repulsion of the electron cloud of monomers A and B, and quantum mechanical effects are not discussed.

Subsequently Morokuma and coworkers[2-4] extended and adapted this decomposition scheme into a rigorous quantum mechanical approach as viewed through the self-consistent-field (SCF) *ab initio* method. There are six components in this decomposition scheme - 1) electrostatic; 2) polarization; 3) exchange repulsion; 4) charge transfer; 5) "MIX"; and 6) "CORR." The CORR term is the contribution of electron correlation which Morokuma and coworkers did not investigate in detail though they stated that the most significant portion of the intermolecular correlation energy is known as the dispersion energy which is an instantaneous effect due to the simultaneous correlation of electrons in monomer A and monomer B. The MIX term is the higher order couplings of the first four components. The polariza-

tion interaction is the distortion of the electron density of A (B) by the presence of monomer B (A) and higher order effects. In applying this decomposition scheme to normal hydrogen-bonded complexes, Umeyama and Morokuma[4] concluded that the binding in these chemical systems is mostly electrostatic in nature with a small but significant contribution from the charge transfer energy.

More recently qualitative approaches based upon electrostatic and polarization interactions have been developed for the theoretical prediction of molecular structures[5,6] and vibrational frequency shifts[7] of hydrogen-bonded complexes. When applied to neutral hydrogen-bonded complexes, both of these methods yield qualitatively correct results, although their accuracy is generally not quantitative and, in some cases, not even semi-quantitative[5-7] . Furthermore, based upon the results of these approaches which have been reported thus far, it seems likely that these classical, perturbative approaches will break down as the binding energy of the complex increases. Since anionic hydrogen-bonded complexes are typically much more strongly bound, these simple approaches are not likely to be as successful.

A more rigorous approach to the study of weakly bound systems which has been applied with much success has been the use of *ab initio* quantum mechanical methods[8] . Numerous studies have demonstrated that the SCF method (coupled with a large one-particle basis set) is capable of describing a weak hydrogen bond reasonably well, except for the dispersion energy. However, the recent formulation and development of better and more efficient electronic structure methods has enabled the direct quantum mechanical investigation of weakly bound molecular complexes at correlated levels of theory. For example, Handy and coworkers[9-12] have determined the equilibrium structures of several weakly bound hydrogen-bonded complexes [HCN···HF, HCN···HCl, $(C_2H_2)_2$, $(C_2H_2)_3$, FH···CO and FH···NNO] using large one-particle basis sets in conjunction with second-order Møller-Plesset perturbation theory (MP2) and have found good agreement with experiment. However, as Rice, Lee and Handy (RLH) have demonstrated[12] with their study of H_2CO···HCl, MP2 is not always adequate, especially when electron correlation effects are very important in the binding of the complex. RLH found that the theoretically more complete coupled-pair functional (CPF) approach gives much better H_2CO and HCl monomer properties and, consequently, the H_2CO···HCl structure is in excellent

agreement with the limited experimental data. In particular the dipole moment of HCl is much better described with the CPF approach, supporting the thesis that electrostatic interactions are important in hydrogen bonding. Nonetheless, the substantial differences in the equilibrium geometry of the $H_2CO\cdots HCl$ complex obtained at the SCF, MP2 and CPF levels of theory demonstrate the importance of the dispersion energy.

Theoretical and experimental studies of anionic hydrogen-bonded complexes are more recent, especially in the gas phase. With the aid of three theoretical studies[13-15] , Kawaguchi and Hirota[16] have recently detected and analyzed the first high resolution infrared (IR) band of an anionic hydrogen-bonded complex (FHF^-). There have been several theoretical studies of anionic hydrogen-bonded complexes, though very few of these have determined equilibrium structures and molecular properties beyond the SCF level of theory. Furthermore, none of the theoretical investigations have studied the decomposition of the hydrogen bond energy of an asymmetric anionic hydrogen-bonded complex. Umeyama *et al.* have performed[17] a decomposition of the hydrogen bond energy of FHF^- and find, not surprisingly, that charge transfer is much more important than for neutral hydrogen-bonded complexes. However, the decomposition analysis of FHF^- is almost certainly not representative of asymmetric systems since FHF^- adopts a $D_{\infty h}$ equilibrium structure.

In some respects anionic hydrogen-bonded complexes provide more of a challenge than neutral and cationic hydrogen-bonded complexes for both experimentalists and theoreticians. For example, the high resolution IR spectroscopist must deal with the very small population of anions that can be generated. Moreover, once a sufficient population has been attained, the analysis of the spectrum is further complicated by the presence of many other ionic species. The difficulty in the *ab initio* study of anionic species is well documented (see for example references 18-23). This difficulty generally arises due to the greater importance of electron correlation in anionic species.

However, in other respects the study of anionic complexes is much easier than the study of similar cationic complexes. From an experimental viewpoint, the large binding energies of anionic hydrogen-bonded complexes should make their gener-

ation an easier task. In order to assess the implications of theoretical studies of anionic complexes, consider $H_5O_2^+$ and $H_3O_2^-$. These two systems are isoelectronic and it is likely that electron correlation effects will be more important for $H_3O_2^-$ than for $H_5O_2^+$. However, $H_3O_2^-$ has two fewer nuclei and therefore six fewer nuclear degrees of freedom. The significant point is that most of the nuclear degrees of freedom which have been eliminated are large amplitude motions, an adequate treatment of which requires knowledge of a large portion of the potential energy surface (PES) as well as a sophisticated treatment of the nuclear motion problem. Existing methods for the accurate determination of the vibrational energy levels of polyatomic species which go beyond the harmonic oscillator approximation and are capable of adequately treating large amplitude motions are highly dependent upon the number of large amplitude nuclear degrees of freedom. Thus, while the description of the electronic structure of anionic hydrogen-bonded complexes is more difficult, the accurate solution of the nuclear motion problem should be more feasible. Therefore, the results of the current study provide data which will ultimately enable the detailed theoretical investigation of molecular systems with several large amplitude nuclear degrees of freedom.

For anionic hydrogen-bonded complexes, the most difficult region of the PES to describe theoretically is the proton transfer coordinate which corresponds to the process $AH + B^- \rightarrow A^- + HB$. The difficulty arises due to the possible existence of two minima corresponding to $A^-\cdots HB$ and $AH\cdots B^-$. Several studies have investigated this region of the PES for symmetric and asymmetric anionic hydrogen-bonded complexes (see for example references 24-27). In addition, one of these[27] also examined the adequacy of various vibrational analysis techniques. These studies have demonstrated that electron correlation effects are vitally important[27] in obtaining a reliable description of the PES along the proton transfer coordinate, and that when A and B are both very electronegative atoms there is generally no barrier (and hence no second minimum) to proton transfer for asymmetric systems[24-27] .

To date, no high level theoretical investigations of anionic hydrogen-bonded complexes involving HF and CN^- or H_2O and CN^- have been reported. Experimentally, the IR spectrum of the M^+FHCN^- ion pair (M^+ being an alkali metal cation) has been studied via matrix isolation techniques by Ault[28] . Fundamental

vibrations were observed in the 1100 cm^{-1} , 1800 cm^{-1} and 2500 cm^{-1} regions and assigned to a bending mode, the proton transfer mode (mostly H-F stretch) and the C-N stretching mode, respectively. Ault also observed that the 1100 cm^{-1} band split into two components which were attributed to the presence of the metal cation M^+. All three modes varied somewhat depending upon the composition of the matrix and the reactants used to form the M^+FHCN^- ion pair. We note that Ault does not seem to have considered the existence of the $FHNC^-$ isomer. Larson, McMahon and Szulejko[24,29] have determined the binding energies (i.e. hydrogen bond strength) of both the $FH\cdots CN^-$ and the $H_2O\cdots CN^-$ complexes. The former is more strongly bound (21.1 kcal/mole) while the latter's binding energy (12.7 kcal/mole) is still much larger than that of a typical neutral hydrogen-bonded complex.

The purpose of this study is to obtain a better understanding of the electron correlation requirements in the *ab initio* study of asymmetric anionic hydrogen-bonded complexes and a more complete understanding of the nature of the bonding present in such systems. Thus, the conclusions of the present study will be useful in deciding upon the level of *ab initio* theory necessary to determine accurately the PES of an anionic hydrogen-bonded complex. The theoretical approach is described in the next section. The following sections contain a presentation and evaluation of our results. Concluding remarks are presented in the final section.

Theoretical Approach

It is well known[18-21] that large basis sets are necessary in order to obtain highly accurate results for anionic systems. Therefore, a single, large one-particle basis set has been used in this study. This basis consists of Dunning's[30] (5s3p) contraction of Huzinaga's[31] [10s6p] Gaussian primitive set for the heavy atoms (C, N, O and F). For hydrogen, the standard (3s) contraction[30] of the [5s] primitive set[31] was used. The hydrogen s function exponents were scaled by a factor of 1.49, as suggested by Dunning. In order to describe better the anionic nature of these systems diffuse s and p functions were added to the heavy atom basis ($\alpha_{s,p}$(C) = 0.04812, 0.03389; $\alpha_{s,p}$(N) = 0.06742, 0.04959; $\alpha_{s,p}$(O) = 0.08993, 0.05840; $\alpha_{s,p}$(F) = 0.1164, 0.07161) while a diffuse s function was included in the hydrogen atomic basis

(α_s(H) = 0.06696). These orbital exponents were determined in an even tempered manner using a method suggested previously[18] . Finally, two sets of polarization functions were added to all the atomic basis sets. The orbital exponents of the d polarization functions are α_d = 1.5, 0.35 for the heavy atoms and α_p = 1.4, 0.25 for hydrogen. These are the values suggested by van Duijneveldt[32] and have been used previously[18] in the study of anionic systems. This basis set is designated TZ2P + diffuse. In all cases, the full complement of six Cartesian d functions was included in the basis giving 110 basis functions for the two larger complexes and 100 basis functions for the two smaller complexes. Linear dependency tests of the one-particle basis set were performed routinely and no problems were encountered.

The first *ab initio* method utilized is the simplest, namely the restricted Hartree-Fock (RHF) SCF technique. As discussed previously, electron correlation effects must be included in order to account for the dispersion energy in hydrogen-bonded complexes. Moreover, it is reasonable to expect that the dispersion energy (or electron correlation effects) will be more important for anionic hydrogen-bonded complexes because of the diffuse, polarizable nature of the electron cloud of anions. Therefore, three different electron correlation methods have been used in order to investigate the importance of electron correlation effects. The first approach is second-order Møller-Plesset perturbation theory[33] (MP2). The second, another commonly used method, is singles and doubles configuration interaction (CISD) which is based upon the variational principle. The third, and theoretically most complete method, is the singles and doubles coupled cluster approach (CCSD). The MP2 and CCSD methods have the advantage of being exactly size extensive and size consistent[34] . The CISD technique includes configuration mixing which MP2 does not take into account, but CISD is an n^6 procedure (MP2 is an n^5 procedure) where n is the number of active molecular orbitals. The CCSD method does allow configuration mixing but is somewhat more expensive than CISD[22] . Also, the energetics of complicated chemical reactions are more easily computed using size consistent methods since "super-molecule" energies are not necessary. Therefore, based upon the above discussion and previous results[35] the CCSD method is expected to yield the most reliable results.

Equilibrium structures of the complexes have been obtained with the SCF,

MP2 and CISD methods. Due to the computational cost and the available computational facilities, at the CCSD level of theory it was only possible to optimize the $FH\cdots CN^-$ and $FH\cdots NC^-$ complexes. However, single point CCSD energies at the MP2 and CISD equilibrium structures have been performed for the $H_2O\cdots CN^-$ and $H_2O\cdots NC^-$ pair of dimers. Also, in order to reduce the CISD expansions the heavy atom 1s-like core molecular orbitals were required to be doubly occupied in all configurations and the corresponding virtual counterpart was deleted from the procedure. The same procedure was also used in the CCSD optimization of the two $FH;CN^-$ complexes.

As noted in the introduction, the structures of many neutral hydrogen-bonded complexes are strongly dependent upon the respective monomer properties. Thus, in an attempt to judge better the reliability of the theoretical predictions of the complexes, all possible monomers have been studied using the basis set and *ab initio* methods described above.

In most cases, analytic energy gradient methods[36] have been employed to locate precisely the equilibrium structures. Analytic energy second derivative methods have been used to determine the SCF[37] and MP2[38,39] Hessian matrices while the CISD and CCSD Hessians were obtained numerically by taking central differences of analytic gradients. Infrared intensities have been determined via the double harmonic approximation. The dipole derivatives were determined analytically at the SCF level of theory and central differences of dipole moments were utilized at the CISD and CCSD levels of theory. In all cases, dipole moments were determined with respect to the center of mass and evaluated as energy derivatives[40] . In the numerical central difference procedures, energy invariance relationships for the Hessian[41] and dipole derivative[42] matrices were used in order to reduce the number of gradient evaluations. This is the most efficient numerical procedure for the evaluation of dipole derivatives provided that the numerical Hessian is also required.

All SCF and MP2 investigations were performed with the Cambridge Analytic Derivatives Package[43] (CADPAC), while the CISD[44,45] and CCSD[46,47] studies were performed with the Berkeley suite of programs modified to run on a Cray X-MP. The CCSD studies of the dimers were performed with a recently developed[22] vectorized CCSD method. SCF, MP2, CISD and monomer CCSD calculations were per-

formed at the University of Cambridge. The CCSD optimizations of $FH\cdots CN^-$ and $FH\cdots NC^-$ were performed on the Cray X-MP/48 at NASA Ames Research Center.

Monomer Properties

The equilibrium structures, total energies and dipole moments of the various monomer fragments are presented in Table 1. The CCSD method provides much better agreement with experimental structures and dipole moments. In fact, for the neutral molecules the magnitude of the errors in the CCSD prediction of the equilibrium structures are less than half those present for the CISD and MP2 structures. The only exception arises for the bond angle in H_2O where the MP2 result is fortuitously in better agreement with the experimental value. However,the CCSD value is only 0.3° too large. Nonetheless, the main conclusions to be drawn from the results of Table 1 are that the CCSD method, as expected, performs better than either the CISD or MP2 approaches and, more importantly, that for many chemical systems quantitatively accurate structures (i.e., $\Delta r_e < 0.001$ Åand $\Delta\Theta_e < 0.5°$) may be obtained with the CCSD electron correlation procedure coupled with a large one-particle basis set.

Another important aspect concerns the equilibrium structure of OH^-. Note that the absolute magnitude of the error of the CCSD bond length is significantly larger than for the A-H (A=C,O,N) bonds of the neutral molecules. The electron correlation energy for anions is generally larger than for isoelectronic neutrals (as evidenced here by comparing the correlation energies of OH^- and H_2O). Thus, anions usually require a more rigorous treatment of electron correlation in order to obtain accuracy comparable to that obtained with neutral molecules. With these considerations, it is not too surprising that the CCSD bond length of OH^- is not as accurate (compared to experiment) as the CCSD O-H bond length in H_2O.

Based upon previous experience, the only other geometrical parameter which is potentially difficult for *ab initio* methods is the C-N triple bond present in CN^-, HCN and HNC. The results given in Table 1 confirm the inherent difficulty in adequately treating the C-N triple bond, though again the CCSD equilibrium values for HCN and HNC are superior to either the CISD or MP2 quantities. For these three molecules, the C-N bond distance decreases in the order $CN^- >$ HNC > HCN,

which yields insight into the nature of the carbon and nitrogen lone pairs. Since the C-N bond distance in CN^- is longer than that in C-N radical, the HOMO exhibits slightly anti-bonding character. Thus, when a proton is attached to form either HCN or HNC the C-N bond distance shrinks due to the polarization of electron density away from the C-N linkage. Therefore, since the C-N distance in HCN is shorter than that found in HNC, we may conclude that C contributes more to the antibonding characteristics than does N. As an aside to the above discussion it is interesting to note that the CISD and CCSD correlation energies for these three molecules increase in magnitude in the order HNC < CN^- < HCN. At the MP2 level of theory the correlation energy of CN^- is slightly larger than that for HCN.

The dipole moments of the monomers are predicted to almost equal accuracy with the CISD or CCSD methods, though the CCSD dipole moment is usually in better agreement with experiment. A noteworthy point which has particular relevance to this study is the fact that the rather sizable dipole moment of CN^- (0.64 D) has carbon at the negative end. Consequently, there are competing effects as to which lone pair of electrons (the C lone pair or the N lone pair) will act as the better Lewis base, or in other words, which end of CN^- will form the stronger hydrogen bond? The nature of these phenomena may be understood by considering electron density maps of the C and N lone pair molecular orbitals which have been given by Taylor *et al.*[47] The C lone pair orbital is broad and diffuse whereas the N lone pair orbital is tighter. Thus, the C lone pair electrons will produce a larger attraction on the proton of the hydrogen-containing monomer in the $AH\cdots CN^-$ complex whereas for the $AH\cdots NC^-$ complex the N nucleus will have a stronger interaction with the electron cloud of the hydrogen-containing monomer since it will be able to approach more closely (i.e. form a shorter hydrogen bond). Thus, it is not evident, *a priori*, which of the two complexes will be more stable. Therefore, if CN^- is one of the monomers of a hydrogen-bonded dimer, it will be necessary to investigate both $AH\cdots CN^-$ and $AH\cdots NC^-$. As we shall demonstrate, for AH being either HF or H_2O both sets of isomers are nearly isoenergetic.

The harmonic vibrational frequencies and infrared (IR) intensities of the monomers are reported in Table 2. As has been noted by several authors recently, the CISD method seems incapable of properly describing the curvature of the PES

around an equilibrium point whereas the size extensive MP2 and CCSD methods both yield quite good harmonic vibrational frequencies. The CISD harmonic frequencies are consistently too high even with the rather large one-particle basis set used in this study. This particular inadequacy with CISD is believed to be related to the lack of size extensivity[49] , though no direct proof has as yet been given.

Somewhat surprisingly the MP2 and CCSD harmonic frequencies are about equally accurate for this set of molecules (with the TZ2P+diffuse basis set), with the CCSD harmonic frequencies for OH^-, HCN and HNC being somewhat better than the MP2 values and the CCSD harmonic frequencies for HF and H_2O being marginally worse than the MP2 quantities. In any case, the MP2 and CCSD harmonic frequencies for the monomers are in very good agreement with experimental values with the possible exception of the bending mode in HCN and HNC. This particular normal mode is very sensitive to specific basis set deficiencies and the interested reader is referred to references 35 and 50 for more details of this effect. Based upon the CCSD and experimental results of the C-N stretching normal mode of HCN and HNC, the experimental harmonic frequency of CN^- can be estimated to lie near 2076 cm^{-1} . Using the $\omega_e x_e$ = 11.3 cm^{-1} determined by Taylor and coworkers[48] , the experimentally unknown fundamental frequency is predicted to lie at 2053 cm^{-1} . This value is in excellent agreement with the high level calculations of Botschwina[51] (2052 $\pm$ 6 cm^{-1}).

The C-N stretch harmonic frequency decreases in the order HCN > CN^- > HNC. Based upon the previously discussed C-N bond distances, the CN^- harmonic frequency would probably have been expected to be the lowest. This result demonstrates that caution must be exercised in relating geometric and vibrational properties.

The IR intensities reported in Table 2 are consistent[52] with the expectation that electron correlation tends to reduce the magnitudes. The CCSD IR intensities demonstrate that while CISD IR intensities are a vast improvement over SCF quantities, the CISD procedure still underestimates the correlation contribution to IR intensities. This observation is entirely consistent with a recent study[49] on the effects of triple and quadruple excitations in the CI electron correlation procedure where it was shown that, like the electronic energy, many molecular properties

tend to converge from one direction as the excitation level is increased (i.e., do not exhibit oscillatory convergence). Thus, based upon the IR intensity and dipole moment data, we may conclude that the CCSD approach better describes the electrical properties of the molecular systems included in this study.

Energetics

In order to determine which dimer will represent the global energy minimum (e.g. $FH\cdots CN^-$ or $F^-\cdots HCN$), it is necessary to consider the enthalpy of the two reactions

$$HF + CN^- + \Delta H_{298} \rightarrow F^- + HCN \qquad (1),$$

and

$$H_2O + CN^- + \Delta H_{298} \rightarrow OH^- + HCN \qquad (2).$$

If ΔH_{298} is positive, then the dimer will correspond to the reactants. Table 3 contains *ab initio* and experimentally derived values for ΔH_{298}. The data in Table 3 clearly indicate that the reactants of equations (1) and (2) should form the more stable dimer. This situation arises due to the large electron affinity of CN and the large F-H and O-H bond energies. Therefore, as discussed above, we must consider two sets of isomers corresponding to hydrogen bond formation through the C or N end of CN^-.

Table 4 contains the total energy, binding energy and dipole moment of each complex, determined at the equilibrium structure for the given level of theory. The most important point to notice is that both sets of isomers are nearly isoenergetic. Thus, it is not possible to say definitively which stationary point represents the lowest energy structure. However, the *ab initio* data are reliable enough to conclude that the actual difference between the isomer's binding energies will not be greater than 5 kcal/mole. Thus, depending upon how the complexes are formed, it is possible that both isomers will be present under a given set of experimental conditions.

The binding energies in Table 4 have incorporated a correction for the basis set superposition error (BSSE). The BSSE was determined using the counterpoise[53] method at the SCF and CCSD levels of theory . It is well established[8] that the BSSE is generally larger at a correlated level of theory and that in order to reduce the

BSSE at a correlated level of theory a very large one-particle basis set is required[8,10] . Therefore, we include the CCSD BSSE for the energetics determined with electron correlation methods.

The best theoretical estimates of the [$H_2O\cdots CN^-$; $H_2O\cdots NC^-$] binding energy (14.5 and 14.7 kcal/mole, respectively) are in good agreement with the experimental[29] value, 12.7 $\pm$ 0.8 kcal/mole. The agreement between theory and experiment for the binding energy of the [$FH\cdots CN^-$; $FH\cdots NC^-$] set of isomers is also good, again being somewhat too large. However, the difference between theory and experiment is somewhat larger for the $FH;CN^-$ pair of complexes. The experimental value may be somewhat too low for this complex and support for this assertion is found by comparing the theoretical and experimental binding energies of the $F^-\cdots H_2O$ complex. A similar[27] level of theory to that used in this study gave a binding energy of 23.2 kcal/mole for $F^-\cdots H_2O$ with the experimental quantity being 23.3 kcal/mole. Thus, the results of this study suggest that the $FH;CN^-$ pair of complexes may be slightly more strongly bound than $F^-\cdots H_2O$, but experimental values suggest the opposite situation. As we shall show, other molecular properties determined via *ab initio* methods (such as the IR intensity of the proton transfer mode) are consistent with the $FH;CN^-$ pair of complexes being more strongly bound.

For both sets of isomers the complex which is hydrogen bonded through the N end of CN^- has a much larger dipole moment. This situation occurs because, in all cases, the negative end of the dipole moment of the dimer is the CN^- end of the complex and so the dipole moment of the complex is greater in magnitude when the negative end of the CN^- moiety is farthest from the center of mass of the dimer. In addition, the difference between the dipole moment of $FH\cdots NC^-$ and $FH\cdots CN^-$ is 0.63 D (CISD), almost exactly the CISD dipole moment of CN^- (0.60 D).

As is usual for hydrogen-bonded complexes, the dipole moment of the complex is greater than the vectorial sum of the two monomers. However, in this case the increase is much larger than normal and is partially due to the charged nature of the complex and the large change in the relationship between the center-of-mass and the center-of-electron charge which occurs upon formation of the complex. Also, the large polarizability of CN^- probably contributes to the sizable dipole moment

of the complexes due to polarization of the CN^- electron cloud away from the HF or H_2O species.

Structures

Table 5 lists the *ab initio* equilibrium structures of the $FH\cdots CN^-$ and $FH\cdots NC^-$ anionic hydrogen-bonded complexes, with those of the $H_2O\cdots CN^-$ and $H_2O\cdots NC^-$ dimers presented in Table 6. See Figures 1 and 2 for the definition of the geometrical parameters contained in Table 6.

For the $FH\cdots CN^-$; $FH\cdots NC^-$ pair of complexes the MP2 level of theory greatly overestimates the effects of electron correlation and CISD underestimates the importance of electron correlation; consistent with the results obtained for the monomers. The CCSD method predicts bond lengths which are between the MP2 and CISD values, but which are much closer to the CISD values than the MP2 quantities. This indicates the importance of electron correlation.

Comparing the complex r_{FH} and r_{CN} with the monomer bond lengths we note that the H-F bond distance increases, as is typical upon hydrogen bond formation, but that the C-N bond distance decreases relative to CN^-. This effect may be due to the loss of some of the C-N antibonding character and is supported by the earlier observation that the C-N distance in CN^- is longer than in either HCN or HNC. This explanation is also consistent with the experimentally observed blue shift in the C-N stretch frequency of $HCN\cdots HF$[54] . Since electron density is drawn away from the C-N bond, the C-N antibonding character is reduced leading to a shorter C-N distance in the complex. The C-N stretch frequency of HCN often exhibits a blue shift in neutral hydrogen bonded complexes[55] .

Interestingly, although the heavy-atom distance ($R_{F..C}$ or $R_{F..N}$) is smaller for $FH\cdots NC^-$ (due to the shorter hydrogen bond), the C-N distance is more affected (relative to CN^-) in $FH\cdots CN^-$. This result tends to suggest that C contributes more to the C-N antibonding characteristics. Another noteworthy feature of the heavy-atom distances, is that for both isomers the CCSD level of theory predicts the largest distances while the MP2 method dramatically underestimates the heavy-atom lengths.

For the $H_2O\cdots CN^-$ and $H_2O\cdots NC^-$ pair of complexes, CCSD geometry opti-

mizations were not possible. However, based upon the above comparisons between CCSD, CISD and MP2 for the FH;CN^- pair, it is reasonable to expect that the CCSD equilibrium structures will be intermediate between the CISD and MP2 optimum geometries and probably somewhat closer to the CISD structures. The various equilibrium structures of the $H_2O\cdots CN^-$ and $H_2O\cdots NC^-$ anionic complexes given in Table 6 exhibit tendencies similar to those reported above for the FH;CN^- pair of dimers. The O-H_1 bond distance (where H_1 is involved in the hydrogen bond, see Figures 1 and 2) elongates upon complexation while the C-N linkage decreases relative to that in CN^-. In addition, the N-H_1 hydrogen bond distance is again shorter than the C-H_1 hydrogen-bond distance; in this case by 0.138 Å. The differential heavy atom distance (i.e., R_{CO} - R_{NO} = 0.1402 Å, CISD) is also larger than for the FH;CN^- pair.

Unique to the H_2O;CN^- complexes is the decrease in the O-H_2 bond distance, the closing of angle γ (see figures 1 and 2 for the definition of γ) and the non-linear hydrogen bond (i.e., A-H$\cdots$B do not lie in a straight line). The decrease in the O-H_2 bond distance seems natural due to the longer O-H_1 distance, though, this result seems to imply that the electron density of the H_2O monomer unit is polarized towards the CN^- monomer unit. While this phenomenon would be expected for neutral hydrogen-bonded complexes, it is not necessarily expected for the case where one of the monomers is an anion. However, the shorter O-H_2 distance may be related to the decrease in the O-H-O angle γ. In other words, long range attractive forces between the H and the electron cloud around the C and/or N will result in a decrease in both r_{O-H_2} and γ. Such long range attractions also explain the non-linear hydrogen bond.

Aside from the hydrogen bond distance and the associated heavy atom distance, the main structural difference between $H_2O\cdots CN^-$ and $H_2O\cdots NC^-$ is the angle α. The smaller angle α for $H_2O\cdots NC^-$ represents a larger deviation from linearity and is consistent with long range attractive forces between H_2 and the electron cloud around C (N in the case of $H_2O\cdots CN^-$). Since the electron density around the C end of CN^- is more diffuse, there is a stronger interaction between H_2 and C in $H_2O\cdots NC^-$ than between H_2 and N in $H_2O\cdots CN^-$. Thus, the angle α is smaller by about 4° for $H_2O\cdots NC^-$.

Diagonalization of the mass-weighted Hessian matrices explicitly demonstrate that each of the four complexes represents a true minimum on the PES. Therefore, attempts were made at the SCF level of theory to locate the transition structure between $FH\cdots CN^-$ and $FH\cdots NC^-$. However, due to the nature of interactions between two closed-shell monomers the potential energy surface is very flat in this region in several degreees of freedom, though the total energy does rise as the CN^- moiety rotates. Performing the full geometry optimization is somewhat complicated and so the actual stationary point structure of the transition state was not pursued further.

A search of the potential energy surface along the proton transfer coordinate was also performed in order to determine whether a second minimum (corresponding to $F^-\cdots HCN$ or $F^-\cdots HNC$) exist. The search along the PES in this coordinate is significantly easier since all the atoms were constrained to be collinear. However, a second minimum (and corresponding transition state) could not be located. A brief discussion of the nature of the PES along the proton transfer coordinate is in order. Generally a transition state (TS) on a PES arises due to an avoided crossing of two states of the same symmetry. Thus, the SCF method is often not an adequate reference function for the TS. However, there are many different types of avoided crossings and in this particular case the SCF wavefunction should be a reasonable reference. This situation arises due to the fact that the orbital occupations of the reactants ($A^-\cdots HB$) and products ($AH\cdots B^-$) are the same. What does occur as the proton is transferred is that two reactant molecular orbitals (a lone pair MO on A^- and a bonding MO in HB) change character and become two product MO's (a lone pair on B^- and a bonding MO in AH). However, since these MO's are of the same symmetry, the transition from reactant to product MO's is smooth along the proton transfer coordinate. We note that the reactant and product MO's belonging to the same irreducible representation is a necessary but not sufficient condition for a smooth transition. Nevertheless, in this specific case the transition from reactant to product MO's appears to be smooth. Therefore, the SCF function should represent a reasonable reference from which to evaluate dynamical electron correlation effects.

Vibrational Spectra

The harmonic vibrational frequencies and infrared intensities for the four anionic hydrogen-bonded dimers included in this study are presented in Table 7. The experimental fundamentals which Ault[28] measured in matrix isolation IR studies are included for comparison, though, because of the rather large anharmonicities which the stretch modes are expected to exhibit, near quantitative accuracy with harmonic frequencies is not possible. The most astonishing result from Table 7 is the variation of the harmonic frequencies ω_1 FH···CN^- and ω_1 FH···NC^- with respect to level of theory. Note that the normal mode associated with ω_1 corresponds to the proton transfer coordinate (i.e., AH···B^- $\rightarrow$ A^-···HB), which for the FH;CN^- complexes is predominately the H-F stretch. Quite clearly, an adequate treatment of electron correlation is extremely important in properly describing the shape of the potential energy surface along this coordinate. Interestingly, the large variations in ω_1 (e.g., for FH···CN^-, 3320 cm^{-1} SCF, 2352 cm^{-1} MP2 and 2844 cm^{-1} CISD) would probably not have been predicted based upon the different equilibrium H-F bond distances (0.947 Å SCF, 1.010 Å MP2, and 0.977 Å CISD), though, not surprisingly, there is a strong correlation between the H-F bond distance and the harmonic frequency. In fact, the nearly linear relationship between $\omega_1$and r_{HF} allows the CCSD ω_1 to be estimated as $\sim$ 2689 cm^{-1} for FH···$CN^-$and $\sim$ 2912 cm^{-1} for FH···NC^-.

Given the large variation of ω_1 with level of theory, it may seem very difficult to arrive at a reliable theoretical prediction for the fundamental band center ν_1. However, studies on similar systems have demonstrated that the individual harmonic frequency and anharmonic correction quantities converge much more slowly (with respect to level of theory) than does the combination, i.e., the fundamental band center. For example, in the study[13] of FHF^- by Janssen *et al.* the harmonic frequency of the antisymmetric stretch ω_3 varies from 627 cm^{-1} to 1538 cm^{-1} while the fundamental ν_3 varies only from 1427 cm^{-1} to 1703 cm^{-1} . A possible explanation for this observation may be that the A···H···B system should be viewed as a particle in a one-dimensional box, where the distance R_{AB} defines the box in which the proton is allowed to move. Thus, we may expect the distance R_{AB} to converge more quickly (with respect to level of theory) than r_{AH} and r_{BH}. In reexamining

the theoretical structures in Table 5 we note that once an iterative electron correlation procedure is used, then the above conditions are met (i.e., $\Delta R < \Delta r$). In any case, the above explanation seems feasible and will no doubt be scrutinized as more theoretical studies concerned with the prediction of the fundamental vibrational frequencies of this type of system are performed.

The second most striking feature of the IR spectrum of the $FH;CN^-$ pair of complexes is the extremely large intensity exhibited by ω_1. Though a large IR intensity is expected for a mode which corresponds to proton transfer, the IR intensities of ω_1 $FH\cdots CN^-$ and ω_1 $FH\cdots NC^-$ are even larger than the IR intensity reported for the analogous mode of $F^-\cdots H_2O$. However, the IR intensity reported for the asymmetric stretch of FHF^- is substantially larger than the ω_1 $FH;CN^-$ quantities. Interestingly, there appears to be a direct correlation between the IR intensity of the proton transer mode and the binding energy of the dimer. The appropriate IR intensity and the *ab initio* binding energy both decrease in the order $FHF^- > FH;CN^- > F^-\cdots H_2O > H_2O;CN^-$. This correlation suggest that the larger the anionic dimer binding energy then the flatter the potential energy surface along the proton transfer coordinate leading to a larger amplitude motion. Of the remaining $FH;CN^-$ normal modes, ω_4 and possibly ω_3 should be observable with ω_2 of $FH\cdots NC^-$ also a possibility. The IR intensities of the $H_2O;CN^-$ pair of complexes are more evenly distributed and, therefore, there are several vibrational modes which should be observable.

For the $H_2O;CN^-$ pair of complexes the proton transfer vibrational mode is ω_2. The variation of ω_2 with respect to level of theory is much smaller than was exhibited by the $FH\cdots CN^-$ and $FH\cdots NC^-$ pair, though it is still substantial. For example, ω_2 for $H_2O\cdots CN^-$ is 3786 cm^{-1} , 3174 cm^{-1} , and 3497 cm^{-1} for the SCF, MP2 and CISD levels of theory, respectively. The smaller variation of ω_2 $H_2O;CN^-$ relative to ω_1 $FH;CN^-$ was, however, to be expected due to the smaller binding energy of the $H_2O;CN^-$ pair.

Another manifestation of the smaller binding energy of the $H_2O\cdots CN^-$, $H_2O\cdots NC^-$ pair of complexes is the lower C-N stretch harmonic frequency relative to the $FH\cdots CN^-$, $FH\cdots NC^-$ pair. As noted previously, the harmonic frequency of CN^- is less than ω_2 in HCN. Thus, in an analogous manner the lower C-N stretch

frequency in the $H_2O;CN^-$ pair is consistent with a smaller interaction between the H_2O and CN^- monomers than exists between the HF and CN^- monomers. These observations also suggest that there is a smaller degree of charge transfer in the $H_2O;CN^-$ complexes than present in the $FH;CN^-$ pair. However, the above observations do not indicate the relative importance of charge transfer in the bonding mechanism.

Not surprisingly, the C-N stretch harmonic frequency of all four complexes exhibits a blue shift relative to the C-N stretch in HCN, CN^- and HNC. As discussed earlier, neutral HCN hydrogen-bonded complexes (such as HF···HCN) often exhibit a blue shift in the C-N stretch due to the loss of C-N antibonding character upon complexation.

By comparing the vibrational spectra of the two $FH;CN^-$ complexes or the $H_2O;CN^-$ pair, it is evident that it would be difficult to distinguish between the two isomers based upon the vibrational frequencies alone. However, due to the differences in their structures, the best method of distinguishing the two isomers will be via analysis of a ro-vibrational band. The rotational constants presented in Table 8 confirm this hypothesis since the differences are well within the accuracy of high resolution spectroscopy.

In order to predict accurately the fundamental band centers of the vibrational modes of these complexes, a potential energy function including very high orders (e.g., octic terms) in some of the degrees of freedom would be required. In addition, a high level approach to the solution of the nuclear Schrödinger equation, which explicitly accounts for large anharmonic couplings, would be necessary. This procedure would obviously be very expensive and is beyond the scope of the present study. However, the vibrational analysis that we have performed has lead to further insight concerning the proton transfer vibrational mode, the most likely fundamental of the $FH;CN^-$ and $H_2O;CN^-$ anionic dimers to be experimentally observed. Furthermore, the similarity of the vibrational spectra of the pairs of isomers has been explicitly demonstrated and a method by which the isomers may be spectroscopically distinguished has been noted.

Bonding

The much larger binding energies found in anionic hydrogen-bonded complexes (relative to neutral hydrogen-bonded complexes) lead to questions concerning the nature of this interaction. For example, if Morokuma and coworkers' hydrogen bond energy decomposition scheme is applied, which components exhibit significantly different characteristics for anionic complexes? As discussed earlier, such an analysis has been performed[17] on FHF^-, however, it seems likely that an asymmetric anionic hydrogen-bonded complex will possess quite different characteristics than FHF^- where charge transfer is clearly very important. Moreover, the binding energy of FHF^- ($\sim$ 39 kcal/mole) is significantly larger than that for the complexes included in this study.

The three hydrogen bond components which one might intuitively expect to yield large attractive energies are the electrostatic, polarization and charge transfer interactions. We will not discuss the electrostatic interactions here except to note that the detailed structure of this interaction must be very different for $FH\cdots CN^-$ ($H_2O\cdots CN^-$) and $FH\cdots NC^-$ ($H_2O\cdots NC^-$) because of the reversal of the dipole moment of CN^-. The total binding energies are very similar, however. Even though the dipole of CN^- has been reversed, this does not mean that the total electrostatic energies of the two isomers are different, though it does seem probable that there will be a detectable difference. In the latter case, some other hydrogen bond energy component must compensate.

The polarization interaction for the anionic hydrogen-bonded complexes included in this study must be significantly larger than exists in a similar neutral hydrogen-bonded complex. This conclusion is based upon the much larger polarizability which anions possess (e.g., at the SCF TZ2P+diffuse level of theory the mean polarizability for HF, H_2O and CN^- is 0.66, 1.14 and 3.48 $Å^3$, respectively). Furthermore, the decomposition analyses which have been performed on neutral[4] and anionic[17] (FHF^-) hydrogen-bonded complexes provide additional support for this inference.

It is difficult to assess the degree of charge transfer. One method would be to perform a Mulliken population analysis on the complex, and from these data determine the number of electrons associated with each monomer. Performing such an analysis on the $FH\cdots CN^-$ and $FH\cdots NC^-$ anionic complexes and comparing to

a similar analysis on the HCN···HF hydrogen bonded complex shows that indeed there is more charge transfer in the anionic species. However, as is well known, a Mulliken population analysis associates electrons to a given nucleus in an ambiguous manner. Therefore, given the rather small differences between the neutral and anionic complexes the validity of the results would seem to be in question. An alternative method would be to perform electron density difference plots between the complexes and their respective monomers and compare these for the anionic and neutral hydrogen-bonded complexes.

Valence electron density difference plots from CISD natural orbitals have been performed for the FH···CN^-, FH···NC^- and HCN···HF hydrogen-bonded complexes and are presented in figures 3 - 5, respectively. The contour interval for all three plots is the same. The HCN···HF equilibrium geometry was taken from reference 9, but the TZ2P+ diffuse basis set of the current study was used. Noting that short dashed lines indicate electron depletion and solid lines indicate an increase in electron density, it is clear that the anionic complexes exhibit a larger charge transfer from the CN^- species to the HF monomer than occurs in the neutral complex. Moreover, this conclusion is enforced by the large buildup of electron density behind the F atom in the anionic complexes. Interestingly, the plots also show a depletion of electron density in the C-N bonding region upon complexation. This observation is entirely consistent with earlier statements concerning the C-N equilibrium bond length and harmonic frequency in HCN, HNC and CN^-.

Considering the above discussion and previous results[2-4,17] , a possible scenerio may be suggested. It is likely that the electrostatic, polarization and charge transfer energy components of an anionic complex are all larger than those for a similar neutral complex. Moreover, as one progesses from an asymmetric complex to a symmetric species (i.e., the proton half way between the heavy atoms), the charge transfer component will become much larger. This model, then, also explains the large difference between the binding energies of FHF^- and FH;CN^-.

Concluding Remarks

The FH···CN^- and FH···NC^- pair of anionic hydrogen-bonded complexes have been shown to be nearly isoenergetic and the theoretical binding energy is in good

agreement with experiment. The $H_2O\cdots CN^-$ and $H_2O\cdots NC^-$ pair of complexes are also very close energetically with the best *ab initio* binding energy again in good agreement with the experimental value. The equilibrium structures of the isomers, however, do exhibit small differences (e.g., the N···H hydrogen bond is shorter than the C···H hydrogen bond) which lead to slightly different rotational constants. Thus, because the harmonic IR spectra of the two pairs of isomers are so similar, the different rotational constants provide a means by which the isomers may be experimentally distinguished. It is concluded, however, that an accurate theoretical determination of the fundamental frequencies will require a large portion of the potential energy surface to be investigated using a high level of electronic structure theory, such as CCSD coupled with a large one-particle basis set. In addition, a sophisticated solution of the nuclear motion problem capable of treating large anharmonicities will be necessary.

Another significant outcome of this study involves the CCSD investigations of the monomers. This is the first study which has fully optimized molecular structures and evaluated several equilibrium molecular properties at the CCSD level of theory with a large one-particle basis set (i.e., larger than double zeta plus polarization) for chemical systems exhibiting a range of bonding characteristics. The CCSD equilibrium structures, harmonic frequencies, dipole moments and IR intensities for HF and H_2O clearly demonstrate that near quantitative results may be obtained for systems which are well described by a single determinant reference function. Although the CCSD results for HCN, HNC, and OH^- have slightly larger errors, they are still very good and are superior to the analogous MP2 and CISD quantities.

Acknowledgements

Parts of this study are based upon work supported by the North Atlantic Treaty Organization under a fellowship awarded to TJL for 1987/1988. The work performed for the ELORET Institute was supported by NASA grant NCC2-552. Professor A. D. Buckingham is thanked for several very interesting and illuminating conversations. Drs. P. R. Taylor, C. W. Bauschlicher and L. A. Barnes are thanked for reading a draft form of this manuscript and making several helpful suggestions.

References

1. Coulson, C. A. *Research* **1957**, *10*, 149.
2. Morokuma, K. *Acc. Chem. Res.* **1977**, *10*, 294.
3. Umeyama, H.; Morokuma, K.; Yamabe, S. *J. Amer. Chem. Soc.* **1977**, *99*, 330.
4. Umeyama, H.; Morokuma, K. *J. Amer. Chem. Soc.* **1977**, *99*, 1316.
5. Buckingham, A. D.; Fowler, P. W. *J. Chem. Phys.* **1983**, *79*, 6426.
6. Buckingham, A. D.; Fowler, P. W. *Can. J. Chem.* **1985**, *63*, 2018.
7. Liu, S.-Y.; Dykstra, C. E. *J. Phys. Chem.* **1986**, *90*, 3097.
8. Van Lenthe, J. H.; van Duijneveldt-van de Rijdt, J. G. C. M.; van Duijneveldt, F. B. *Ab Initio Methods in Quantum Chemistry* **1987**, Vol. 2, pp. 521-566.
9. Amos, R. D.; Gaw, J. F.; Handy, N. C.; Simandiras, E. D.; Somasundram, K. *Theor. Chim. Acta* **1987**, *71*, 41.
10. Alberts, I. L.; Rowlands, T. W.; Handy, N. C. *J. Chem. Phys.* **1988**, *88*, 3811.
11. Alberts, I. L.; Handy, N. C.; Simandiras, E. D. *Theor. Chim. Acta* **1988**, *74*, xxxx.
12. Rice, J. E.; Lee, T. J.; Handy, N. C. *J. Chem. Phys.* **1988**, *88*, 7011.
13. Janssen, C. L.; Allen, W. D.; Schaefer, H. F.; Bowman, J. M. *Chem. Phys. Lett.* **1986**, *131*, 352.
14. Yamashita, K.; Morokuma, K. (unpublished work, quoted in reference 12)
15. Botschwina, P. (unpublished work, quoted in reference 12)
16. Kawaguchi, K.; Hirota, E. *J. Chem. Phys.* **1987**, *87*, 6838.
17. Umeyama, H.; Kitaura, K.; Morokuma, K. *Chem. Phys. Lett.* **1975**, *36*, 11.
18. Lee, T. J.; Schaefer, H. F. *J. Chem. Phys.* **1985**, *83*, 1784.
19. Radom, L. in *Methods of Electronic Structure Theory* edited by H. F. Schaefer (Plenum, New York, 1977), Vol. 4, pp. 333-352.
20. Clark, T.; Chandrasekhar, J.; Spitznagel, G. W.; Schleyer, P. v. R. *J. Comput. Chem.* **1983**, *4*, 294.
21. Simons, J.; Jordan, K. D. *Chem. Rev.* **1987**, *87*, 535.
22. Lee, T. J.; Rice, J. E. *Chem. Phys. Lett.* **1988**, *150*, 406.

23. Radom, L. *Aust. J. Chem.* **1976**, *29*, 1635.
24. Larson, J. W.; McMahon, T. B. *J. Amer. Chem. Soc.* **1983**, *105*, 2944.
25. Cybulski, S. M.; Scheiner, S. *J. Amer. Chem. Soc.* **1987**, *109*, 4199.
26. Cybulski, S. M.; Scheiner, S. *J. Amer. Chem. Soc.* **1989**, *111*, 23.
27. Yates, B. F.; Schaefer, H. F.; Lee, T. J.; Rice, J. E. *J. Amer. Chem. Soc.* **1988**, *110*, 6327.
28. Ault, B. S. *J. Phys. Chem.* **1979**, *83*, 2634.
29. Larson, J. W.; Szulejko, J. E.; McMahon, T. B. *J. Amer. Chem. Soc.* **1988**, *110*, 7604.
30. Dunning, T. H. *J. Chem. Phys.* **1971**, *55*, 716.
31. Huzinaga, S. *J. Chem. Phys.* **1965**, *42*, 1293.
32. Van Duijneveldt, F. B. *IBM Res. Dept. RJ* **1971**, 945.
33. Møller, C.; Plesset, M. S. *Phys. Rev.* **1934**, *46*, 618.
34. Bartlett, R. J.; Purvis, G. D. *International J. Quant. Chem. Symp.* **1978**, *14*, 561.
35. See for example, Simandiras, E. D.; Rice, J. E.; Lee, T. J.; Amos, R. D.; Handy, N. C. *J. Chem. Phys.* **1988**, *88*, 3187.
36. Pulay, P. *Mol. Phys.* **1969**, *17*, 197.
37. Pople, J. A.; Krishnan, R.; Schlegel, H. B.; Binkley, J. S. *International J. Quant. Chem. Symp.* **1979**, *13*, 225.
38. Handy, N. C.; Amos, R. D.; Gaw, J. F.; Rice, J. E.; Simandiras, E. D.; Lee, T. J.; Harrison, R. J.; Laidig, W. D.; Fitzgerald, G.; Bartlett, R. J. in *Geometrical Derivatives of Energy Surfaces and Molecular Properties* edited by P. Jorgensen and J. Simons (Reidel, Dordrecht, 1986).
39. Simandiras, E. D.; Amos, R. D.; Handy, N. C. *Chem. Phys. Lett.* **1987**, *114*, 9.
40. Diercksen, G. H. F.; Roos, B. D.; Sadlej, A. J. *Chem. Phys.* **1981**, *59*, 29.
41. Page, M.; Saxe, P.; Adams, G. F.; Lengsfield, B. H. *Chem. Phys. Lett.* **1984**, *104*, 587.
42. Lee, T. J. Ph. D. thesis, University of California, Berkeley, 1986.
43. Amos, R. D.; Rice, J. E. CADPAC: Cambridge Analytic Derivatives Package, Issue 4.0, 1988.

44. Saxe, P.; Fox, D. J.; Schaefer, H. F.; Handy, N. C. *J. Chem. Phys.* **1982**, *77*, 5584.
45. Rice, J. E.; Amos, R. D.; Handy, N. C.; Lee, T. J.; Schaefer, H. F. *J. Chem. Phys.* **1986**, *85*, 963.
46. Scuseria, G. E.; Scheiner, A. C.; Lee, T. J.; Rice, J. E.; Schaefer, H. F. *J. Chem. Phys.* **1987**, *86*, 2881.
47. Scheiner, A. C.; Scuseria, G. E.; Rice, J. E.; Lee, T. J.; Schaefer, H. F. *J. Chem. Phys.* **1987**, *87*, 5361.
48. Taylor, P. R.; Bacskay, G. B.; Hush, N. S.; Hurley, A. C. *J. Chem. Phys.* **1979**, *70*, 4481.
49. Lee, T. J.; Remington, R.B.; Yamaguchi, Y.; Schaefer, H. F. *J. Chem. Phys.* **1988**, *89*, 408.
50. Taylor, P. R.; Almlöf, J.; Sellers, H.; Saebø, S.; McLean, A. D. to be published.
51. Botschwina, P. *Chem. Phys. Lett.* **1985**, *114*, 58.
52. Yamaguchi, Y.; Frisch, M. J.; Gaw, J. F.; Schaefer, H. F.; Binkley, J. S. *J. Chem. Phys.* **1986**, *84*, 2262.
53. Boys, S. F.; Bernardi, F. *Mol. Phys.* **1970**, *19*, 553.
54. Wofford, B. A.; Bevan, J. W.; Olson, W. B.; Lafferty, W. J. *J. Chem. Phys.* **1985**, *83*, 6188.
55. See for example, Hopkins, G. A,; Maroncelli, M.; Nibler, J. W.; Dyke, T. R. *Chem. Phys. Lett.* **1985**, *114*, 97.
56. Huber, K. P.; Herzberg, G. *Constants of Diatomic Molecules* (Van Nostrand Reinhold, New York, 1979).
57. Muenter, J. S.; Klemperer, J. *J. Chem. Phys.* **1970**, *52*, 6033.
58. Owrutsky, J. C.; Rosenbaum, N. H.; Tack, L. M.; Saykally, R. J. *J. Chem. Phys.* **1985**, *83*, 5338.
59. Hoy, A. R.; Bunker, P. R. *J. Mol. Spectrosc.* **1979**, *74*, 1.
60. Clough, S. A.; Beers, Y.; Klein, G. D.; Rothman, L. S. *J. Chem. Phys.* **1973**, *59*, 2254.
61. Winnewisser, G.; Maki, A. G.; Johnson, D. R. *J. Mol. Spectrosc.* **1971**, *39*, 149.
62. Ebenstein, W. L.; Muenter, J. S. *J. Chem. Phys.* **1984**, *80*, 3989.

63. Creswell, R. A.; Robiette, A. G. *Mol. Phys.* **1978**, *36*, 869.
64. Blackman, G. L.; Brown, R. D.; Godfrey, P. D.; Gunn, H. I. *Nature* **1976**, *261*, 395.
65. Pine, A. S.; Fried, A.; Elkins, J. W.; *J. Mol. Spectrosc.* **1985**, *109*, 30.
66. Hoy, A. R.; Mills, I. M.; Strey, G. *Mol. Phys.* **1972**, *24*, 1265.
67. Ziles, B. A.; Person, W. B. *J. Chem. Phys.* **1983**, *79*, 65.
68. Quapp, W. *J. Mol. Spectrosc.* **1987**, *125*, 122.
69. Hyde, G. E.; Hornig, D. F. *J. Chem. Phys.* **1952**, *20*, 647.
70. Electron affinities and bond energies taken from the 68th edition of the CRC Handbook of Chemistry and Physics, Editor R. C. Weast, CRC Press Inc. 1987-1988.
71. Del Bene, J. E.; Mettee, H. D.; Frisch, M. J.; Luke, B. T.; Pople, J. A. *J. Phys. Chem.* **1983**, *87*, 17.

Figure Captions

Figure 1. Definition of the internal coordinates for the $H_2O\cdots CN^-$ anionic hydrogen-bonded complex.

Figure 2. Definition of the internal coordinates for the $H_2O\cdots NC^-$ anionic hydrogen-bonded complex.

Figure 3. Valence electron density difference plot for the $FH\cdots CN^-$ anionic complex. Short dashed lines indicate a depletion of electron density while solid lines indicate an increase of electron density.

Figure 4. Valence electron density difference plot for the $FH\cdots NC^-$ anionic complex. Short dashed lines indicate a depletion of electron density while solid lines indicate an increase of electron density.

Figure 3. Valence electron density difference plot for the $HCN\cdots HF$ hydrogen-bonded complex. Short dashed lines indicate a depletion of electron density while solid lines indicate an increase of electron density.

Table 1
Theoretical predictions of the total energy, optimum structure and dipole moment of the possible fragmentation monomers. Energies, bond lengths, angles and dipole moments are given in Hartrees, Å, degrees and Debyes respectively.

Monomer	Structure		Method	Energy	Dipole Moment
F^-			SCF	-99.455226	-
			MP2	-99.724127	-
			CISD	-99.691431	-
			CCSD	-99.718898	-
HF	r_{HF}	0.8985	SCF	-100.064599	1.89
		0.9208	MP2	-100.317487	-
		0.9149	CISD	-100.293761	1.82
		0.9176	CCSD	-100.319608	1.81
		0.9168	Expt[a]	-	1.80
OH^-	r_{OH}	0.9426	SCF	-75.413857	1.35
		0.9655	MP2	-75.688586	-
		0.9580	CISD	-75.654436	1.25
		0.9624	CCSD	-75.685247	1.24
		0.9643	Expt[b]	-	-
CN^-	r_{CN}	1.1513	SCF	-92.342662	0.46
		1.1870	MP2	-92.695252	-
		1.1688	CISD	-92.637209	0.60
		1.1744	CCSD	-92.698406	0.64
		-	Expt	-	-
H_2O	r_{OH}	0.9404	SCF	-76.062199	1.95
	∠HOH	106.4°			
	r_{OH}	0.9593	MP2	-76.315821	-
	∠HOH	104.5°			
	r_{OH}	0.9540	CISD	-76.293736	1.89
	∠HOH	105.0°			
	r_{OH}	0.9571	CCSD	-76.321837	1.88
	∠HOH	104.8°			
	r_{OH}	0.9578	Expt[c]	-	1.85
	∠HOH	104.5°			

Table 1 continued

Monomer	Structure		Method	Energy	Dipole Moment
HCN	r_{HC}	1.0572	SCF	-92.909715	3.27
	r_{NC}	1.1235			
	r_{HC}	1.0641	MP2	-93.262244	-
	r_{NC}	1.1637			
	r_{HC}	1.0618	CISD	-93.207319	3.08
	r_{NC}	1.1438			
	r_{HC}	1.0653	CCSD	-93.268033	3.03
	r_{NC}	1.1502			
	r_{HC}	1.065	Expt[d]	-	2.99
	r_{NC}	1.153			
HNC	r_{HN}	0.9819	SCF	-92.892533	2.97
	r_{CN}	1.1440			
	r_{HN}	0.9959	MP2	-93.233324	-
	r_{CN}	1.1733			
	r_{HN}	0.9903	CISD	-93.185062	3.09
	r_{CN}	1.1609			
	r_{HN}	0.9939	CCSD	-93.244549	3.11
	r_{CN}	1.1658			
	r_{HN}	0.9940	Expt[e]	-	3.05
	r_{CN}	1.1689			

a. All experimental structures refer to derived equilibrium structures. HF bond length from Ref [56] and dipole moment from Ref [57].
b. Ref [58].
c. Structure from Ref [59] and dipole moment from Ref [60].
d. Structure from Ref [61] and dipole moment from Ref [62].
e. Structure from Ref [63] and dipole moment from Ref [64].

Table 2
Harmonic vibrational frequencies and infrared intensities
for the monomers. Frequencies are given in cm^{-1} and IR intensities
(in parentheses) in km/mol.

Monomer	Normal mode	SCF	MP2	CISD	CCSD	Expt
HF	$\omega_1(\sigma)$	4469 (164)	4126	4212 (114)	4165 (106)	4139 (96)[a]
CN^-	$\omega_1(\sigma)$	2317 (45)	1982	2167 (21)	2112 (16)	-
OH^-	$\omega_1(\sigma)$	4073 (62)	3805	3855 (77)	3782 (85)	3738[b]
H_2O	$\omega_1(a_1)$	4130 (15)	3841	3919 (6)	3865 (4)	3832 (2)[c]
	$\omega_2(a_1)$	1757 (96)	1657	1694 (74)	1684 (71)	1649 (54)
	$\omega_3(b_2)$	4233 (92)	3967	4021 (62)	3972 (57)	3942 (45)
HCN	$\omega_1(\sigma)$	3608 (72)	3451	3497 (68)	3438 (64)	3442 (59)[d]
	$\omega_2(\sigma)$	2407 (11)	2027	2236 (2)	2171 (0.4)	2129 (0.2)
	$\omega_3(\pi)$	855 (70)	686	734 (72)	706 (72)	727 (50)
HNC	$\omega_1(\sigma)$	4046 (379)	3818	3899 (286)	3839 (260)	3842[e]
	$\omega_2(\sigma)$	2282 (103)	2017	2145 (70)	2098 (62)	2067
	$\omega_3(\pi)$	472 (313)	459	425 (277)	442 (269)	490

a. All experimental frequencies are derived harmonic frequencies. The harmonic frequency is taken from ref [56] while the IR intensity is taken from ref [65].
b. The harmonic frequency is taken from ref [58].
c. The harmonic frequencies are taken from ref [66] while the IR intensities are taken from ref [67].
d. The harmonic frequencies are taken from ref [68] while the IR intensities are taken from ref [69].
e. The harmonic frequencies are taken from ref [63].

Table 3

Thermochemical data for possible fragmentation products of the titled anionic hydrogen bonded complexes in kcal/mole.

Method	ΔH_{298} [a,c]	ΔH_{298} [b]
SCF	27	50
MP2	17	36
CISD	21	42
CCSD[d]	20	41
Expt[e]	26	45

a) $HF + CN^- + \Delta H_{298} \rightarrow F^- + HCN$

b) $H_2O + CN^- + \Delta H_{298} \rightarrow OH^- + HCN$

c) Difference in total electronic energies, zero point vibrational energies and rotational and translational contributions at 298K.

d) The CCSD values use the CISD zero point vibrational energies.

e) Ref [70].

Table 4

Predicted binding energies (kcal/mol) and dipole moments (Debyes) for the anionic hydrogen bonded complexes. The binding energies were computed with respect to the most stable dissociation products as indicated in Table 3.

Anionic complex	Method	Energy	ΔE^a	ΔE^b	Dipole Moment
FH···CN^-	SCF	-192.442703	22.1	22.0	2.92
	MP2	-193.056400	27.8	26.8	-
	CISD	-192.940474	25.3	24.3	2.38
	CCSD[c]	-193.059361	25.5	24.5	-
FH···NC^-	SCF	-192.444070	23.0	22.9	3.19
	MP2	-193.054960	26.1	25.0	-
	CISD	-192.940721	25.4	24.3	3.01
	CCSD[c]	-193.059157	25.4	24.3	-
	Expt[d]	-	-	21.1	-
H_2O···CN^-	SCF	-168.424382	12.4	12.3	4.29
	MP2	-169.036450	16.3	15.6	-
	CISD	-168.920387	14.5	13.8	3.84
	CCSD[e]	-169.043811	15.2	14.5	-
H_2O···NC^-	SCF	-168.425723	13.4	13.4	4.48
	MP2	-169.036487	16.2	15.4	-
	CISD	-168.921256	15.1	14.3	4.32
	CCSD[e]	-169.044430	15.5	14.7	-
	Expt[f]	-	-	12.7±0.8	-

a. Includes zero point energy and translational, rotational correction for 298K, see ref 71 for method.
b. Includes zero point energy and translational, rotational correction and basis set superposition error determined by the counterpoise method, ref 53.
c. CCSD energy performed at CCSD equilibrium geometry. The single point energy allowed all orbitals to be active, whereas in the geometry optimization the core and corresponding virtual orbitals were frozen. The optimum CCSD energies are -193.004605 and -193.004374 for FH···CN^- and FH···NC^-, respectively. CISD zero point energies were used.
d. Ref 24.
e. CCSD energy at the CISD equilibrium geometry. All orbitals active in the CCSD procedure. CISD zero point energies were used.
f. Ref 29.

Table 5
Geometrical structures for the anionic hydrogen bonded complexes $FH\cdots CN^-$ and $FH\cdots NC^-$. Bond lengths are given in Å.

Anionic complex	Method	r_{FH}	r_{CN}	$r_{H\ldots C}$	$R_{F\ldots C}$
$FH\cdots CN^-$	SCF	0.9472	1.1457	1.7790	2.7262
	MP2	1.0103	1.1803	1.6039	2.6142
	CISD	0.9769	1.1585	1.6768	2.6537
	CCSD	0.9879	1.1696	1.6666	2.6546
		r_{FH}	r_{CN}	$r_{H\ldots N}$	$R_{F\ldots N}$
$FH\cdots NC^-$	SCF	0.9437	1.1483	1.6481	2.5918
	MP2	0.9898	1.1820	1.5460	2.5358
	CISD	0.9678	1.1611	1.5798	2.5476
	CCSD	0.9768	1.1719	1.5785	2.5553

Table 6
Geometrical structures for the anionic hydrogen bonded complexes $H_2O\cdots CN^-$ and $H_2O\cdots NC^-$. See Figure 2 for definitions of the molecular bond angles. Bond lengths are given in Å and bond angles in degrees.

Anionic complex	Method	r_{OH_1}	r_{OH_2}	r_{CN}	$r_{C\cdots H_1}$	R_{CO}	α	β	γ
$H_2O\cdots CN^-$	SCF	0.9599	0.9392	1.1484	2.1246	3.0706	176.3°	168.2°	103.6°
	MP2	0.9966	0.9586	1.1836	1.9055	2.8984	176.8°	173.9°	102.0°
	CISD	0.9769	0.9486	1.1614	1.9903	2.9601	176.6°	171.5°	102.7°
		r_{OH_1}	r_{OH_2}	r_{CN}	$r_{N\cdots H_1}$	R_{NO}	α	β	γ
$H_2O\cdots NC^-$	SCF	0.9596	0.9390	1.1500	1.9501	2.8963	173.0°	168.3°	103.6°
	MP2	0.9914	0.9581	1.1847	1.8012	2.7885	172.8°	173.6°	102.2°
	CISD	0.9749	0.9484	1.1629	1.8523	2.8199	172.3°	171.4°	102.8°

Table 7

Harmonic vibrational frequencies and infrared intensities
for the anionic hydrogen bonded complexes.
Frequencies are given in cm^{-1} and IR intensities (in parentheses) in km/mole .

Anionic Complex	Normal mode	SCF	MP2	CISD	Expt.[a]
FH···CN^-	$\omega_1(\sigma)$	3320 (2203)	2352	2844 (2679)	1800
	$\omega_2(\sigma)$	2373 (21)	2044	2261 (7)	2500
	$\omega_3(\sigma)$	246 (46)	298	278 (61)	-
	$\omega_4(\pi)$	1043 (190)	1142	1107 (143)	1100
	$\omega_5(\pi)$	162 (3)	159	163 (3)	-
FH···NC^-	$\omega_1(\sigma)$	3406 (2271)	2727	3034 (2618)	1800
	$\omega_2(\sigma)$	2346 (101)	2030	2235 (74)	2500
	$\omega_3(\sigma)$	276 (58)	309	300 (70)	-
	$\omega_4(\pi)$	1034 (254)	1104	1086 (211)	1100
	$\omega_5(\pi)$	123 (5)	127	126 (8)	-
H_2O···CN−	$\omega_1(a')$	4195 (43)	3911	4050 (28)	
	$\omega_2(a')$	3786 (801)	3174	3497 (1106)	
	$\omega_3(a')$	2345 (30)	2012	2232 (12)	
	$\omega_4(a')$	1822 (114)	1722	1777 (88)	
	$\omega_5(a')$	406 (73)	472	446 (66)	
	$\omega_6(a')$	175 (26)	217	202 (32)	
	$\omega_7(a')$	96 (3)	93	98 (3)	
	$\omega_8(a'')$	798 (116)	902	860 (84)	
	$\omega_9(a'')$	115 (13)	106	114 (10)	
H_2O···NC^-	$\omega_1(a')$	4198 (43)	3919	4054 (30)	
	$\omega_2(a')$	3800 (864)	3289	3548 (1116)	
	$\omega_3(a')$	2329 (74)	2004	2216 (50)	
	$\omega_4(a')$	1827 (127)	1730	1782 (100)	
	$\omega_5(a')$	398 (73)	463	439 (66)	
	$\omega_6(a')$	197 (34)	237	225 (41)	
	$\omega_7(a')$	71 (4)	75	72 (5)	
	$\omega_8(a'')$	802 (133)	890	856 (101)	
	$\omega_9(a'')$	90 (30)	96	93 (33)	

a. Experimental fundamental frequencies are taken from ref [28].

Table 8

Rotational Constants (MHz) for the Equilibrium structures of the Anionic Complexes.

Anionic Complex	SCF	MP2	CISD	CCSD
$FH\cdots CN^-$				
A	3825	4021	3966	3946
$FH\cdots NC^-$				
A	4348	4438	4443	4404
$H_2O\cdots CN^-$				-
A	513050	536470	530720	
B	3370	3631	3548	
C	3348	3607	3524	
$H_2O\cdots NC^-$				-
A	455610	469440	455490	
B	3887	4065	4033	
C	3854	4031	3998	

Figure Captions

Figure 1. Definition of the internal coordinates for the $H_2O\cdots CN^-$ anionic hydrogen-bonded complex.

Figure 2. Definition of the internal coordinates for the $H_2O\cdots NC^-$ anionic hydrogen-bonded complex.

Figure 3. Valence electron density difference plot for the $FH\cdots CN^-$ anionic complex. Short dashed lines indicate a depletion of electron density while solid lines indicate an increase of electron density.

Figure 4. Valence electron density difference plot for the $FH\cdots NC^-$ anionic complex. Short dashed lines indicate a depletion of electron density while solid lines indicate an increase of electron density.

Figure 5. Valence electron density difference plot for the $HCN\cdots HF$ hydrogen-bonded complex. Short dashed lines indicate a depletion of electron density while solid lines indicate an increase of electron density.

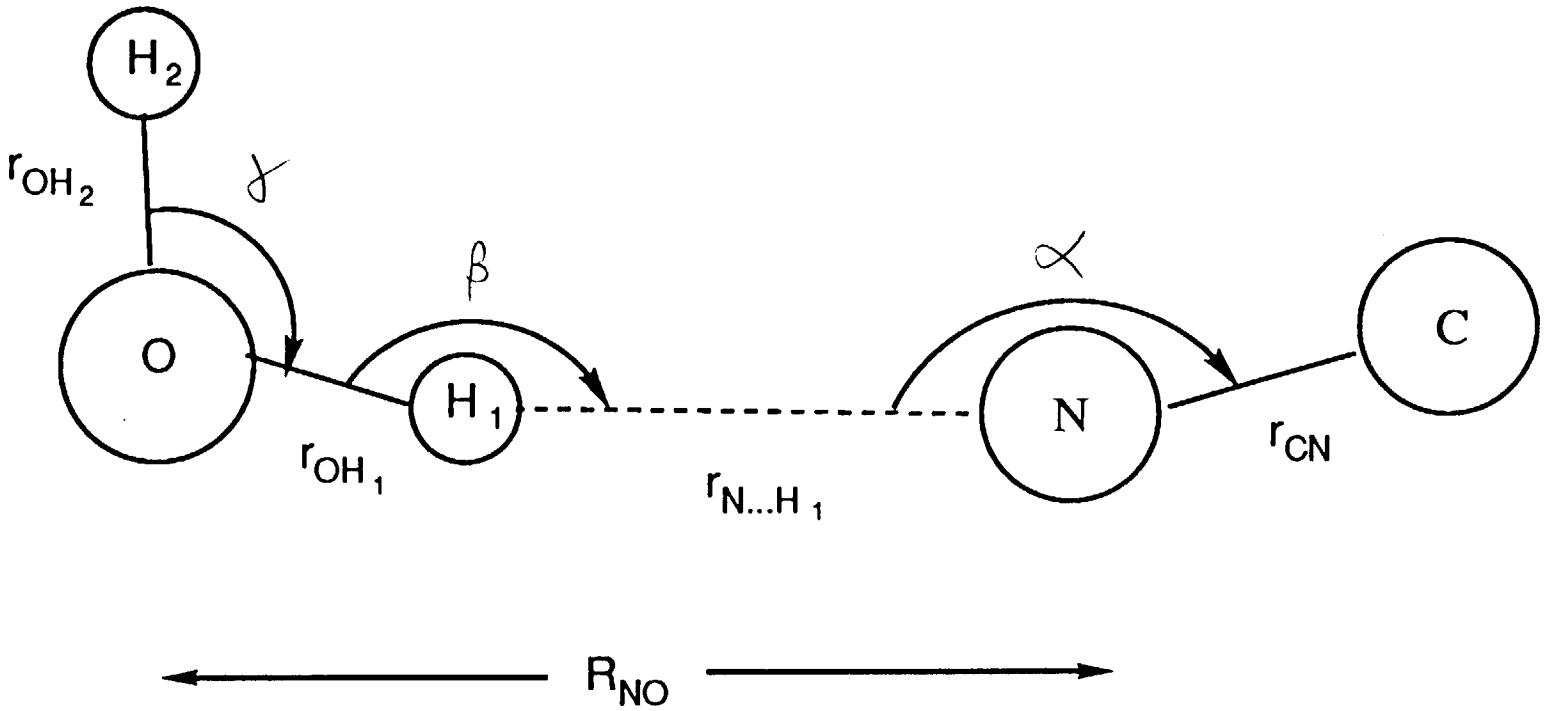
H2
rOH2
γ
β
α
O
H1
N
C
rOH1
rN...H1
rCN
RNO

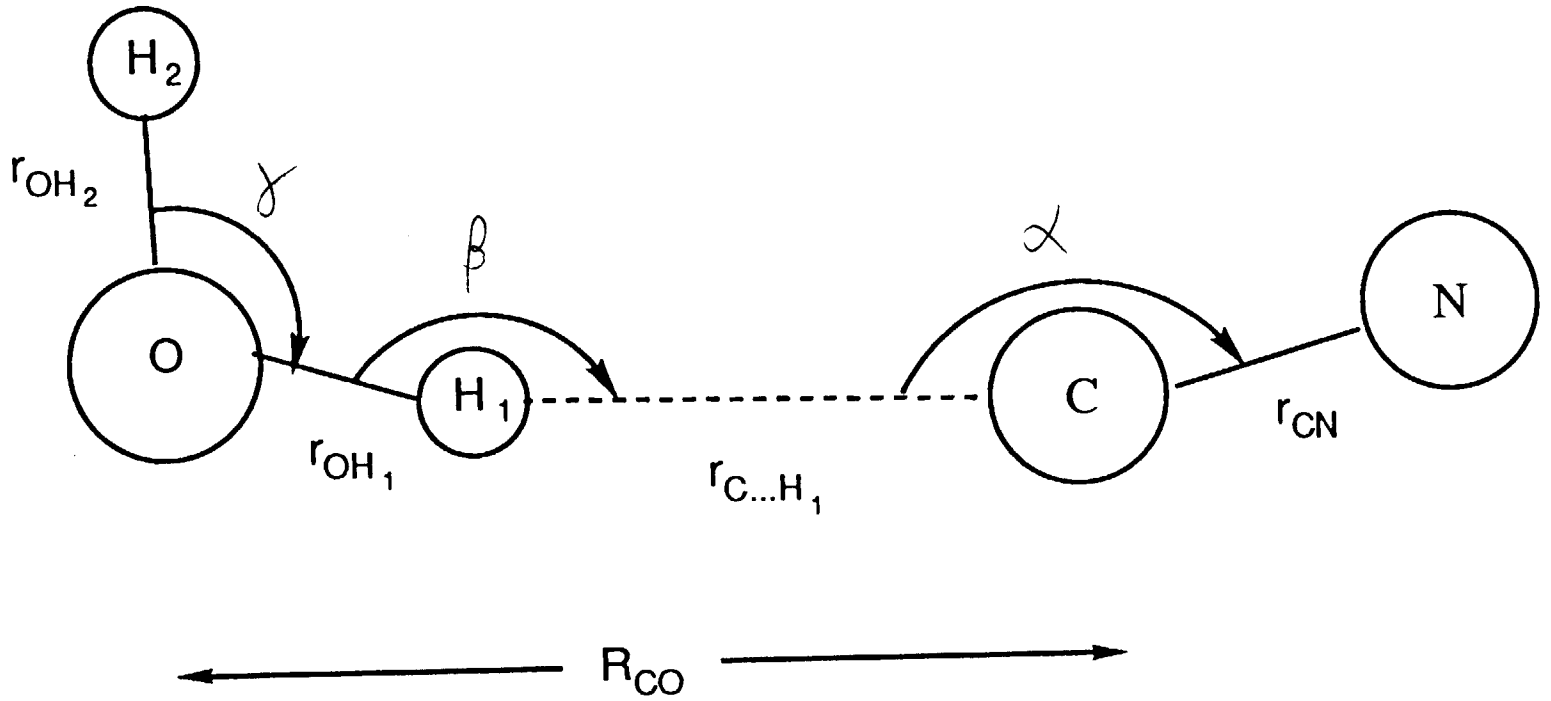
H2
rOH2
γ
β
α
O
H1
C
N
rOH1
rC...H1
rCN
RCO

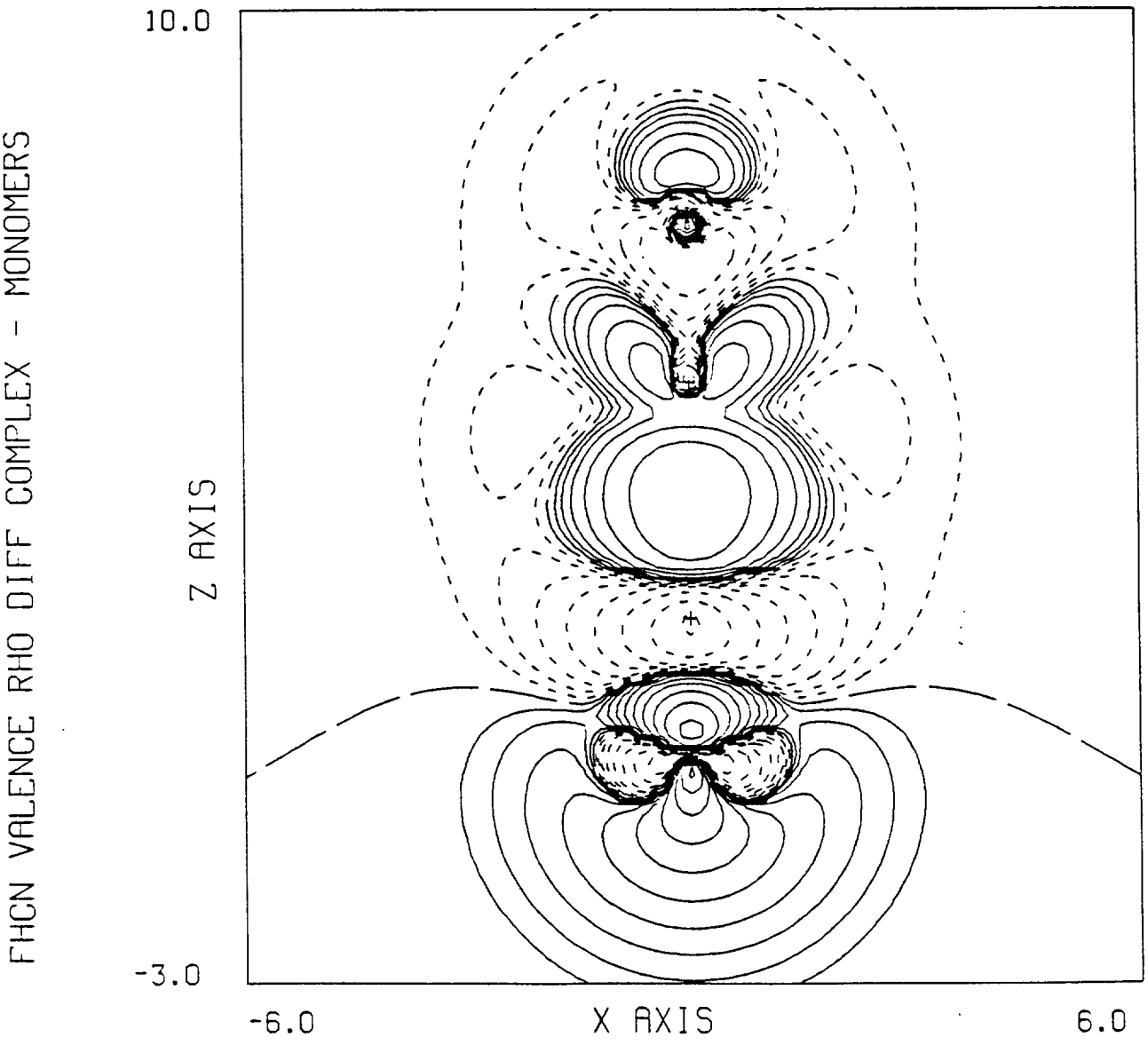
FHCN VALENCE RHO DIFF COMPLEX - MONOMERS
10.0
Z AXIS
-3.0
-6.0
X AXIS
6.0

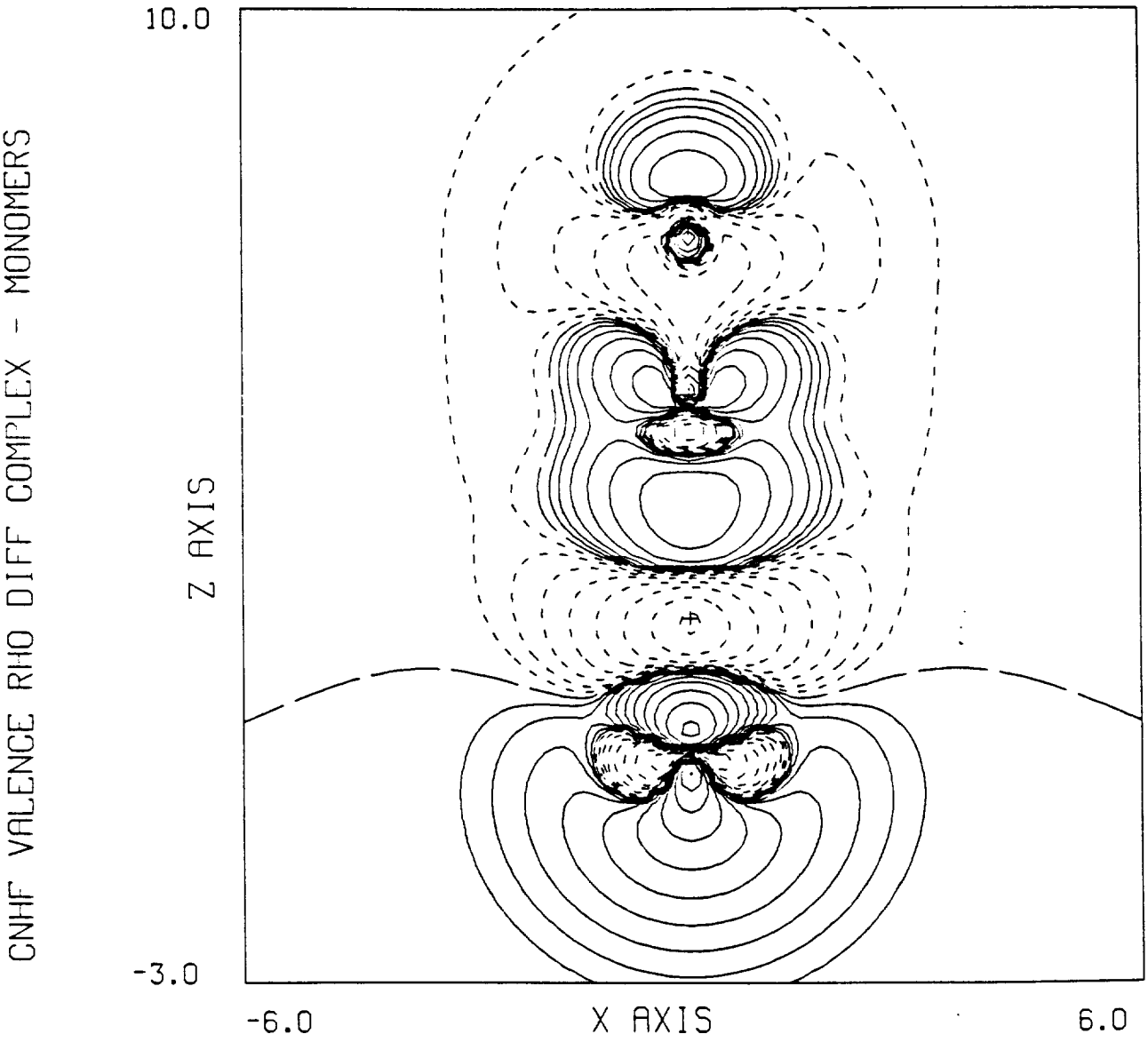
CNHF VALENCE RHO DIFF COMPLEX - MONOMERS
10.0
Z AXIS
-3.0
-6.0
X AXIS
6.0

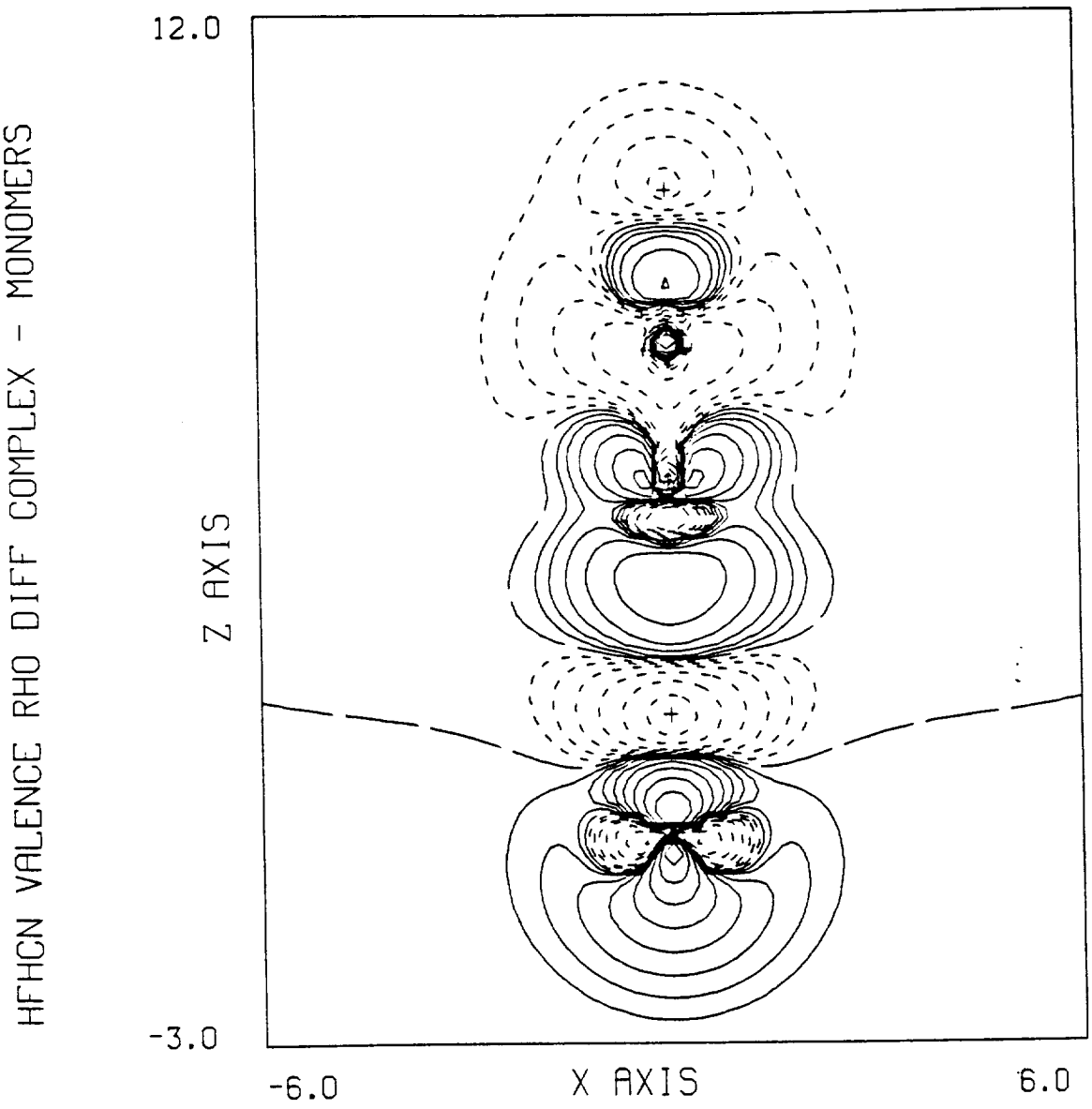
HFHCN VALENCE RHO DIFF COMPLEX - MONOMERS
12.0
-3.0
Z AXIS
-6.0
X AXIS
6.0